

1 **Single amino acid mutation decouples photochemistry of the BLUF domain from the enzymatic  
2 function of OaPAC and drives the enzyme to a switched-on state**

3 Jinnette Tolentino Collado<sup>1#</sup>, Emoke Bodis<sup>2#</sup>, Jonatan Pasitka<sup>2</sup>, Mihaly Szucs<sup>2</sup>, Zsuzsanna Fekete<sup>2</sup>,  
4 Nikolett Kis-Bicskei<sup>2</sup>, Elek Telek<sup>2</sup>, Kinga Pozsonyi<sup>2</sup>, Sofia M. Kapetanaki<sup>2</sup>, Greg Greetham<sup>3</sup>, Peter J.  
5 Tonge<sup>\*1</sup>, Stephen R. Meech<sup>\*4</sup>, and Andras Lukacs<sup>\*2</sup>

6 <sup>1</sup> Department of Chemistry, Stony Brook University, New York, 11794, United States.

7 <sup>2</sup> Department of Biophysics, Medical School, University of Pecs, Szigeti str. 12, 7624 Pecs, Hungary.

8 <sup>3</sup> Central Laser Facility, Research Complex at Harwell, Rutherford Appleton Laboratory, Didcot, OX11 0QX, U.K

9 <sup>4</sup> School of Chemistry, University of East Anglia, Norwich, NR4 7TJ, U.K.

10 <sup>#</sup> Equally contributed

11 <sup>\*</sup> Correspondence: [andras.lukacs@aok.pte.hu](mailto:andras.lukacs@aok.pte.hu); [s.meech@uea.ac.uk](mailto:s.meech@uea.ac.uk); [peter.tonge@stonybrook.edu](mailto:peter.tonge@stonybrook.edu)

12

13 **Abstract**

14 Photoactivated adenylate cyclases (PACs) are light-activated enzymes that combine a BLUF (blue-light  
15 using flavin) domain and an adenylate cyclase domain that are able to increase the levels of the important  
16 second messenger cAMP (cyclic adenosine monophosphate) upon blue-light excitation. The light-induced  
17 changes in the BLUF domain are transduced to the adenylate cyclase domain via a mechanism that has not  
18 yet been established. One critical residue in the photoactivation mechanism of BLUF domains, present in  
19 the vicinity of the flavin is the glutamine amino acid close to the N5 of the flavin. The role of this residue  
20 has been investigated extensively both experimentally and theoretically. However, its role in the activity of  
21 the photoactivated adenylate cyclase, OaPAC has never been addressed. In this work, we applied ultrafast  
22 transient visible and infrared spectroscopies to study the photochemistry of the Q48E OaPAC mutant. This  
23 mutation altered the primary electron transfer process and switched the enzyme into a permanent ‘on’ state,  
24 able to increase the cAMP levels under dark conditions compared to the cAMP levels of the dark-adapted  
25 state of the wild-type OaPAC. Differential scanning calorimetry measurements point to a less compact  
26 structure for the Q48E OaPAC mutant. The ensemble of these findings provide insight into the important  
27 elements in PACs and how their fine tuning may help in the design of optogenetic devices.

28

29

## 1      **Introduction**

2      OaPAC is a photoactivated adenylate cyclase (PAC) discovered recently in the cyanobacteria  
3      *Oscillatoria acuminata* that translates a blue-light signal into the production of cyclic adenosine  
4      monophosphate (cAMP) [1]. OaPAC is a homodimer of a 366-aa protein comprising an N-terminal BLUF  
5      (blue-light sensing using FAD) domain and a C-terminal class III adenylyl cyclase (AC) domain. The basal  
6      activity of OaPAC is very low under dark conditions, but under light conditions it is stimulated up to 20-  
7      fold, making OaPAC a very good candidate for optogenetic applications [1].

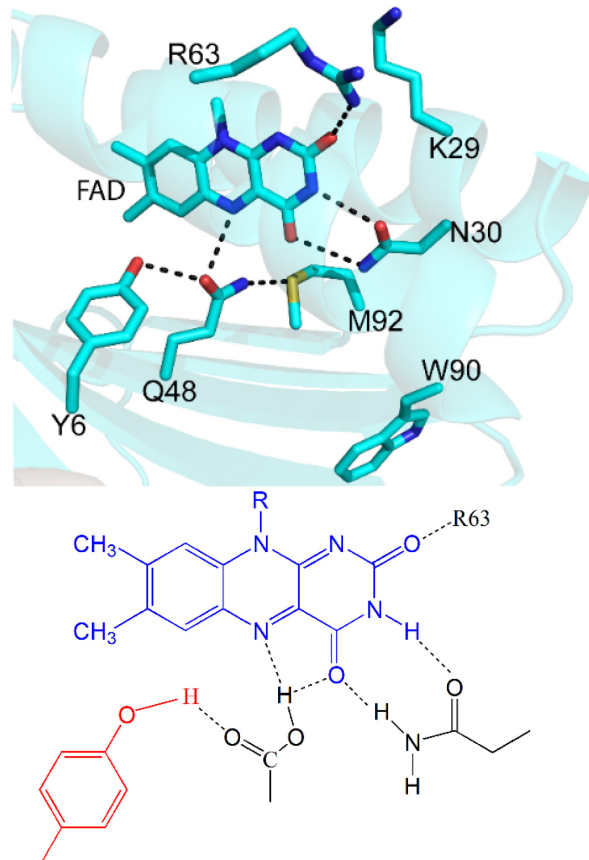
8      PACs have captured the interest of biologists in the past two decades after the discovery of EuPAC, the  
9      first member of the family found in the unicellular flagellate, *Euglena gracillis*, in which the step-up  
10     photophobic response is mediated by the cyclase activity[2]. In the majority of PACs the light dependent  
11     production of cAMP is controlled by a BLUF domain located at the N-terminal of the protein [2]. PACs  
12     exploit the photochemistry of the BLUF domain to transmit a light-induced downstream signal that  
13     enhances the cAMP levels [3, 4]. All BLUF proteins work using the same elegant mechanism: blue light  
14     absorption of the flavin leads to a rearrangement of the hydrogen bond network around the flavin and this  
15     primary structural change propagates through the protein leading to intramolecular conformational changes  
16     at the C-terminal that regulates the activity of the protein or can even control interprotein interactions[5-  
17     10]. In our earlier work, using time-resolved multiple probe spectroscopy (TRMPS) we were able to follow  
18     the propagation of the signal in the BLUF domain of Activator of the Photopigment and pucA (AppA) by  
19     monitoring the structural changes occurring in the  $\beta$ -sheet within 20  $\mu$ s of light absorption [11].

20     The photochemistry of BLUF domains depends on the conserved amino acid residues around the  
21     isoalloxazine ring[12-17] (Fig. 1). A close-lying tyrosine (conserved in all BLUF domains) serves as both  
22     an electron and a proton donor. Another key amino acid residue which is also conserved in all BLUF  
23     domains is the glutamine residue close to the N5 atom of the flavin. The role of glutamine (Q48 in OaPAC,  
24     Q63 in AppA, Q50 in PixD) in the photoactivation of BLUF domain proteins has been extensively  
25     investigated, as it was observed that it is necessary for transmitting the structural change from the BLUF  
26     domain towards the C-terminal part of the protein [16, 18-20]. Replacement of this amino acid residue  
27     resulted in the loss of the characteristic spectral red-shift observed in BLUF domain proteins upon blue  
28     light irradiation [21, 22]. The group of Bauer was the first to replace the glutamine residue Q63 in AppA  
29     with a glutamic acid and they have observed a ~3nm red shift (from 446 nm to 449.5 nm) of the S<sub>0</sub>-S<sub>1</sub>  
30     transition of the flavin in the Q63E AppA mutant [21]. Based on this observation and fluorescence

1 spectroscopy experiments they proposed that the Q63E AppA mutant is in lit mode. An early model,  
2 deduced from the first crystal structure of AppA [23], proposed that the glutamine side chain rotates after  
3 photoexcitation. Based on transient infrared experimental data and quantum chemical calculations it was  
4 proposed that a photoinduced keto-enol tautomerization of the close glutamine (Q63) to the N5 atom of  
5 flavin leads to the ultrafast reorganization of the hydrogen bond network [16, 24]. Quantum chemical  
6 calculations show that the driving force for this is an electron transfer reaction [25, 26] mediated by  
7 structural relaxation where Y6 is the primary electron donor, but W90 can donate an electron as well, as in  
8 the WT protein we observed the formation of the anionic flavin radical ( $\text{FAD}^{\bullet-}$ ) at early times after  
9 excitation but only the neutral flavin radical was formed in the W90F mutant [4]. Based on our time resolved  
10 infrared (TRIR) and visible transient absorption (TA) measurements[4] we proposed that the primary  
11 photochemistry of OaPAC is the following: tyrosine Y6 gives an electron and a proton at the same time  
12 (concerted forward proton -coupled electron transfer, PCET) to the oxidized flavin to form the semiquinone  
13 flavin ( $\text{FADH}^{\bullet}$ ) in  $\sim$ 24 ps. In less than 200 ps,  $\text{FADH}^{\bullet}$  decays to the signalling state of the flavin via a  
14 reverse electron and proton transfer to the tyrosine Y6. This signalling state is characterized by the well-  
15 known red-shift of the S0-S1 transition and of the C4=O carbonyl stretch of the flavin in the absorption and  
16 infrared spectra, respectively. The flavin remains in this signalling state for  $\sim$  5s, and the ATP- cAMP  
17 conversion happens during this time. However, there is an open question on the nature of the hydrogen  
18 bond reorganization around the flavin and how this rearrangement is transduced to the AC domain of  
19 OaPAC.

20 It should be pointed out that the radical intermediate states mentioned above for the flavin and the tyrosine  
21 residue have been identified in some BLUF domains (but not in AppA), by their characteristic markers in  
22 ultrafast visible and infrared measurements [4, 25-29] whereas the forward PCET step has been reported to  
23 be sequential in PixD[25-27] . Regardless of the sequence of the PCET reaction (concerted or sequential),  
24 the conserved glutamine residue is considered crucial for the propagation of the signal from the BLUF  
25 domain to the effector domain with the keto-enol tautomerization being the focus of many experimental  
26 and theoretical studies in AppA and PixD[22, 28-33]. In particular, very recently Hontani *et al* [34] revisited  
27 the tautomerization models in PixD by means of femtosecond stimulated Raman spectroscopy (FSRS),  
28 isotope labelling and computational methods and they revisited the models proposed (in the case of AppA)  
29 for the light activation. The authors concluded that the Anderson[13, 35] model which proposed the rotation  
30 of this specific glutamine residue cannot be used to explain the experimental data. They also proposed that  
31 the Sadeghian/Stelling[16, 36] model which proposed to form a tautomer in the light adapted state but  
32 without rotating its side chain does not fit their observation neither. Hontani et al. concluded that after

1 photoexcitation glutamine tautomerizes to the imidic form which is followed by a sidechain rotation to  
2 form the light adapted state.  
3



4  
5 **Figure1** A) Environment of FAD in OaPAC (pdb:4yus) showing the residues involved in the hydrogen bond network around  
6 the flavin. Glutamine is hydrogen bonded to the flavin, the tyrosine and the methionine before excitation. B) Possible  
7 orientation of E48 and hydrogen bonds to the flavin.  
8

9 In a recent ultrafast absorption study Chen et al.[37] have studied bidirectional proton relay using the triple  
10 OaPAC BLUF mutant Y6WQ48EW90F and have decoupled the forward electron transfer and the proton  
11 transfer from tyrosine Y6 to the flavin. The results obtained allowed them to propose a Grotthus mechanism  
12 [38]—a proton transfer along a hydrogen bond – taking place during the protonation of the flavin by Q48E.  
13 Despite the intense interest in the role of the glutamine residue on BLUF domains, there are no studies  
14 addressing the potential effect of the glutamine mutation on the effector domain in BLUF and PAC proteins.  
15 The studies mentioned above have been performed on the BLUF domains and not on the full-length  
16 proteins. To investigate the implications of the glutamine residue on the enzymatic activity of OaPAC, we  
17 have studied the functional dynamics of the full-length Q48E OaPAC mutant using ultrafast transient  
18 visible and infrared spectroscopies and contrasted them with the functional dynamics of the wild-type full-

1 length OaPAC. The glutamine to glutamic acid mutation is an interesting one as it removes the possibility  
2 of either an asymmetry in the rotation or the formation on the imine tautomer while offering the potential  
3 of retaining the H-bond structure around the flavin ring.

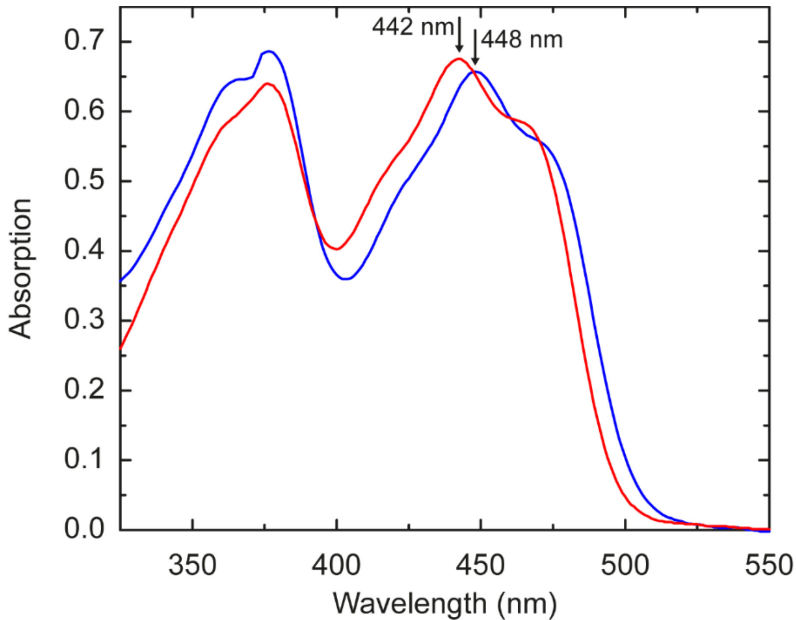
4 As in OaPAC the photosensor domain and the effector domain are part of the same protein – contrary to  
5 the AppA-PpsR complex – it was a straightforward idea to study the effects of this mutation on the  
6 functional activity of the protein.

7 As expected, the Q48E mutation indeed suppresses photoactivity. We have also shown that it significantly  
8 affects the structure of the enzyme, as indicated by differential scanning calorimetry measurements. Our  
9 findings support a proton coupled electron transfer pathway in the Q48E OaPAC mutant. In addition,  
10 enzymatic assays suggest that replacement of the glutamine by the glutamic acid locks the protein in a  
11 ‘switched-on’ state that decouples the adenylate cyclase domain from the BLUF domain and converts ATP  
12 to cAMP in a light- independent manner. Comparisons with the analogous mutation in PixD<sub>BLUF</sub> (Q50E)  
13 are made and the implications of our results on the engineering of PACs for optogenetic applications are  
14 discussed.

15

## 16 **Results and discussion**

17 The absorption spectrum of the Q48E OaPAC mutant shows a significant difference to the absorption  
18 spectrum of the wild-type enzyme, with the maximum of the visible flavin absorption attributed to the S<sub>0</sub>-  
19 S<sub>1</sub>  $\pi$ - $\pi^*$  transition of the isoalloxazine moiety [39] at 448 nm red-shifted by 6 nm compared to the wild-  
20 type (Fig. 2). Since the characteristic dark to light 10-15 nm red-shift of the specific flavin transition in  
21 BLUF domains originates from a hydrogen bond rearrangement around the flavin, it can be postulated that  
22 the observed 6 nm red-shift of the absorption maximum in the Q48E OaPAC mutant arises from a mutation  
23 induced change in the hydrogen bond network around the flavin. It is worth mentioning that the analogous  
24 Q63E mutation in AppA<sub>BLUF</sub> resulted in a smaller red-shift (3 nm) [22]. Similar to the Q63E AppA mutant,  
25 blue-light irradiation of the Q48E OaPAC mutant does not result in a further red-shift of the maximum  
26 absorption of the flavin, indicating that the Q48E OaPAC mutant is photoinactive.



1

2 Fig. 2 Absorption spectra of the dark-adapted states of the wild-type OaPAC (red line) and the Q48E  
 3 OaPAC mutant (blue line). The absorption maximum is red shifted in the Q48E mutant suggesting a  
 4 change in the surrounding hydrogen bonding network of the flavin.

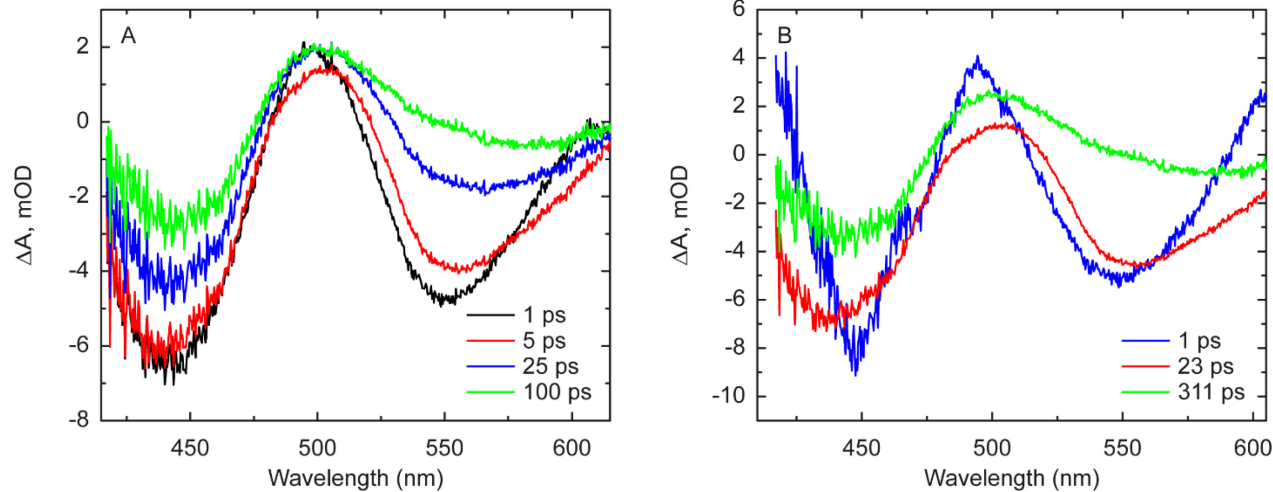
5 *Transient absorption measurements*

6 To characterize the early steps of the photochemistry of the Q48E OaPAC mutant, we applied ultrafast  
 7 transient absorption spectroscopy. Transient absorption spectra of BLUF domain proteins are dominated  
 8 by the spectral properties of the flavin chromophore; the transient absorption spectrum has three salient  
 9 features: a negative  $\Delta A$  (called bleach) in the spectral region (400-500 nm) where the flavin absorbs ( $S_0-S_1$   
 10 transition), a positive peak (excited state absorption, ESA) near 500 nm and a broad negative band at  $>530$   
 11 nm attributed to stimulated emission (SE). Global analysis of the data, assuming a sequential kinetic model  
 12 revealed a heterogeneous decay with three decay constants (1 ps, 23 ps, 311 ps). The transient absorption  
 13 spectra of the Q48E (Figure 3A) do not show any obvious components which can be assigned to the  
 14 formation of radical intermediates which have distinct spectral features (see Fig. S5,  $\text{FADH}^\bullet$  has a broad  
 15 absorption in the 500-700 nm range,  $\text{FAD}^\bullet$  has a distinct peak at 400 nm). The evolution associated  
 16 difference spectra (EADS, Fig. 3B) also did not resolve a clear radical intermediate although spectral  
 17 modelling of the 311 ps component show the presence of the  $\text{FADH}^\bullet$  species (see Fig S5. C) This may  
 18 reflect an overlap with the SE and ESA or that any radical population is low due to kinetic considerations;  
 19 the spectra of the radical species have been proven elusive in other BLUF domains. However, the fact that  
 20 the excited  $\text{FAD}^*$  state decays in hundreds of picoseconds points to an effective quenching which could be

1 the result of an electron transfer to the excited flavin, otherwise FAD\* would have a longer lifetime ( $\sim 4$   
2 ns) [28].

3

4



5

6 Fig. 3 A) Comparison of transient absorption spectra of the Q48E mutant at the indicated time delays. The spectra are  
7 dominated by a bleach around 450 nm, excited state at  $\sim 500$  nm and simulated emission in the  $\sim 520$ - $570$  nm region B) EADS  
8 spectra obtained after the global analysis show a heterogeneous decay of the excited state.

9

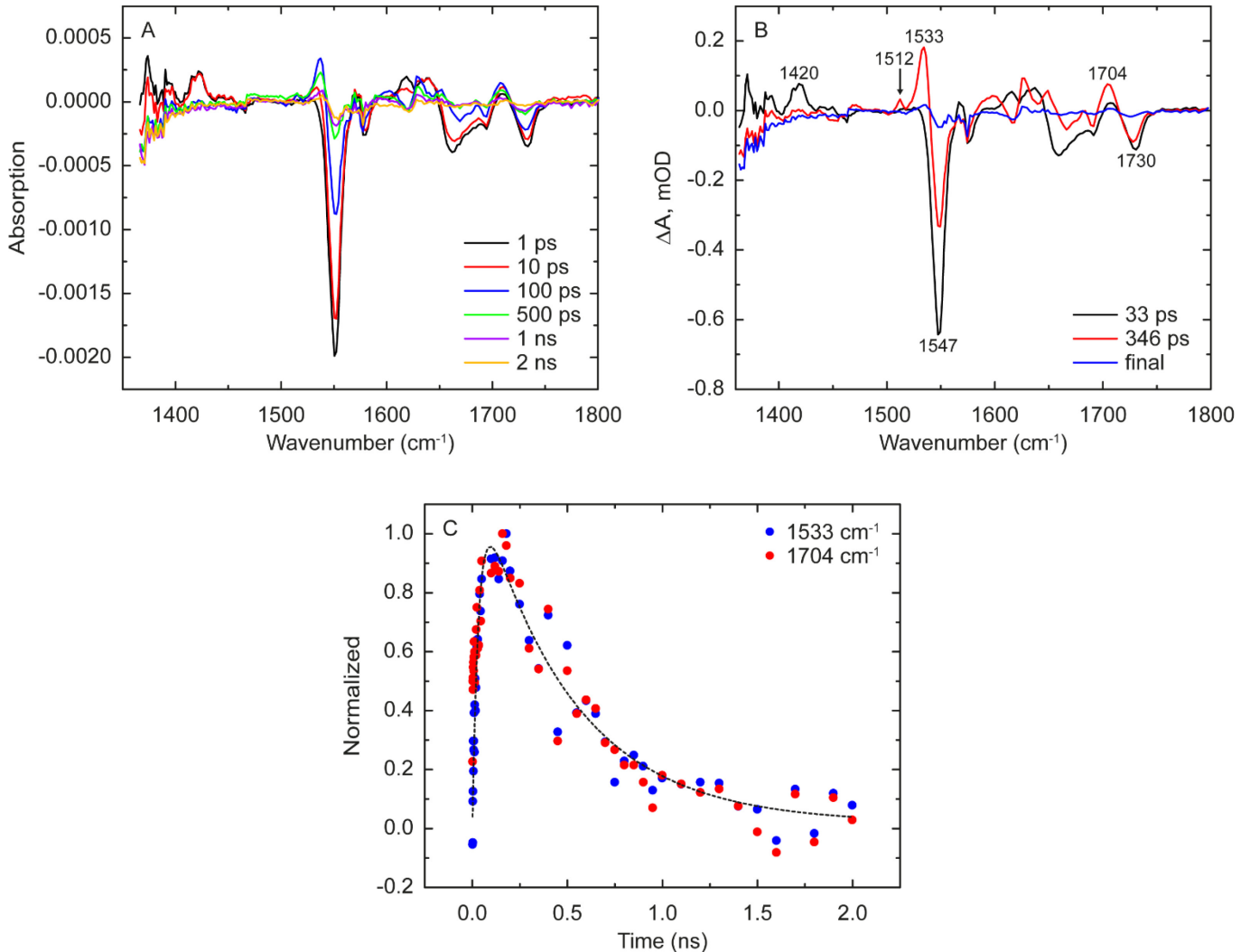
10

### 11 *Transient infrared absorption measurements*

12 To obtain a more detailed picture on the nature of the flavin intermediates as well as of the changes  
13 occurring in the protein vibrational spectra following blue-light excitation, we performed time-resolved  
14 infrared spectroscopy (TRIR). Figure 4A shows the temporal evolution of the TRIR spectra of the dark-  
15 adapted state of the Q48E OaPAC mutant after blue-light excitation. The most salient features of the TRIR  
16 spectra observed at 10 ps after excitation are related to the flavin vibrational modes and are similar to those  
17 observed in the wild-type OaPAC [4]. The intense bleach at  $1547\text{ cm}^{-1}$  and the weaker one at  $1581\text{ cm}^{-1}$  are  
18 well known flavin adenine dinucleotide (FAD) ring modes [29-33]. The most significant differences  
19 compared to the TRIR spectra of wild-type OaPAC (Fig. S2) are the negative peak observed at  $1730\text{ cm}^{-1}$ ,

1 the positive peak at  $1704\text{ cm}^{-1}$  and a negative bleach around  $1690\text{ cm}^{-1}$ . In the wild-type enzyme a bleach  
2 is observed at  $1704\text{ cm}^{-1}$  assigned to the bleached FAD ground state carbonyl. This significant difference  
3 at the higher frequencies is the result of a mutation-induced change in the hydrogen bond network around  
4 the flavin as explained below. In our earlier work [22] on the analogous Q63E mutation in AppA we showed  
5 using isotope labelling that the new bleach (at  $1724\text{ cm}^{-1}$  in AppABLUF) does not originate from a flavin  
6 vibrational mode but from the side chain of the glutamic acid. Moreover, this high-frequency band ( $1724\text{ cm}^{-1}$   
7 in Q63E AppA and  $1730\text{ cm}^{-1}$  in Q48E OaPAC) is observed in the expected absorption range of  
8 protonated carboxylic acids ( $1700\text{--}1770\text{ cm}^{-1}$ ) [40-44] and therefore can be assigned to the vibrational mode  
9 of a protonated carboxylic acid side chain of the glutamic acid. The presence of the  $\sim 1690\text{ cm}^{-1}$  bleach  
10 indicates that the carbonyl at the C4 atom of FAD forms a hydrogen bond with the glutamic acid already at  
11 the moment of excitation (see Fig 1B). The exact same peak is formed in the wild-type OaPAC 184 ps  
12 after excitation and has been assigned to a downshifted C4=O group ( $1704\text{ cm}^{-1}$  in the ground-state) of the  
13 glutamine residue due to an additional hydrogen bond to it [4]. The origin of the positive  $1704\text{ cm}^{-1}$  peak is  
14 more complex: it could be assigned to the vibration of the protonated carbonyl of E48 but can partially arise  
15 from the C4=O carbonyl and is discussed in more detail below.

16 The EADS of the TRIR for the Q48E mutant are shown in Fig.4B. Assuming a sequential model, global  
17 analysis of the TRIR data reveals two components with lifetimes 33ps, 346 ps and a third constant  
18 component with an infinite lifetime. The first EADS spectrum can be assigned to the difference spectrum  
19 of the oxidized flavin; the  $1420\text{ cm}^{-1}$  peak is a vibrational marker of the flavin S<sub>1</sub> excited state [17].  
20 Comparison of the relaxation of the excited state ( $1420\text{ cm}^{-1}$ ) and the ground state recovery observed  $1547\text{ cm}^{-1}$   
21 (Fig. S1 A) shows that the time constant of the excited state decay is significantly faster than that of  
22 the ground state recovery, pointing to the formation of intermediates during the ground state recovery  
23 process [17]. These can be identified as radical intermediates in EADS2, where one can observe the  
24 formation of three distinct peaks at  $1512\text{ cm}^{-1}$ ,  $1533\text{ cm}^{-1}$  and  $1704\text{ cm}^{-1}$ . The appearance of the peak at  
25  $1533\text{ cm}^{-1}$  suggests the formation of a neutral flavin radical FADH<sup>•</sup> in 33ps, as this peak is a known  
26 vibrational marker of the neutral flavin radical [4, 45]. The  $1512\text{ cm}^{-1}$  peak forms with the same time  
27 constant (Fig. S1 B) and we have previously assigned this to a vibrational mode of the neutral tyrosyl [4,  
28 45], its formation with the same time constant indicates the formation of the Y6<sup>•</sup> radical simultaneously  
29 with the formation of the FADH<sup>•</sup> radical.



1  
2 Fig. 4 A) Transient infrared spectra of the Q48E mutant at the indicated time delays B) EADS spectra from the global analysis  
3 performed on the transient infrared data C) Kinetics observed at  $1533\text{ cm}^{-1}$  and  $1704\text{ cm}^{-1}$  (the sign of the latter is inverted for  
4 comparison).

5  
6 The kinetics of the  $1533\text{ cm}^{-1}$  peak (the protonation of the flavin,  $\text{FADH}^{\cdot}$ ) share the same time constant (~  
7  $33\text{ ps}$ ) with the rise of the  $1704\text{ cm}^{-1}$  mode (Fig. 4C).

8 Based on theoretical calculations on Slr 1694 (PixD) [26] a double proton transfer was proposed for the  
9 photoactivation of OaPAC [4, 46, 47]: after photoexcitation the tyrosine gives an electron to the flavin and  
10 a proton to the glutamine (Q48) and the glutamine protonates the flavin forming the  $\text{FADH}^{\cdot}$  intermediate.  
11 This concerted PCET mechanism differs from the sequential mechanism observed for the Y6WW90FQ48E  
12 OaPAC mutant reported by Chen et al. [37]. In their study, they assigned a fast proton transfer (3.8 ps in  
13 water) from the glutamic acid to the anionic flavin radical, followed by a slower proton transfer (336 ps in  
14 water) from the tryptophan cation radical to the deprotonated glutamic acid. This difference is not  
15 surprising, as the  $\text{p}K_{\text{a}}$  of the tyrosine cation radical is significantly lower (~ -2)[48] than that of the

1 tryptophan cation radical ( $\sim 4$ )[49], justifying a faster deprotonation step for the tyrosine. It should be  
2 pointed out that the fast deprotonation of the tyrosine is the reason that the formation of the tyrosine cation  
3 radical has been observed by ultrafast spectroscopy in only a few systems [50-52]. The 346 ps EADS shows  
4 the radical recombination reaction to largely recover the original ground state.

5 The two TRIR EADS must be compared to the three from the TA, requiring an assignment of the  
6 additional 1 ps component appearing only in the latter. This could indicate a vibrational relaxation in the  
7 excited state as the  $\sim 5000 \text{ cm}^{-1}$  excess energy in the 400 nm excitation is dissipated, modifying the shape  
8 of the transient electronic spectra. Such a relaxation of the hot electronically excited state need not have a  
9 signature in the transient IR spectra, where in any case the excess energy is less due to the 450 nm excitation  
10 used. Alternatively, an ultrafast charge separation and recombination reaction could occur in a  
11 subpopulation of the protein that is not detected in TRIR. Both calculation and experiment in other BLUF  
12 domains point to a distribution of ground state structures and inhomogeneous decay kinetics[6, 53, 54] .  
13 Thus, a population with exceptionally fast charge separation and recombination may exist. Such an  
14 unproductive photocycle might not be resolved in the lower time resolution and signal to noise of TRIR.

15 For the remaining two EADS, there is reasonable agreement between the two time constants recovered  
16 (33 and 346 ps from TRIR and 23 and 311 ps in TA). However, even here the two components are not  
17 obviously due to the same underlying processes. For example the 33 ps TRIR appears to show complete  
18 decay of the FAD\* state ( $1420 \text{ cm}^{-1}$ ). However the longer lives EADS in TA data shows both SE and ESA  
19 components, consistent with some longer lived population in FAD\*. Similarly, the TRIR EADS at  $1547 \text{ cm}^{-1}$   
20 shows significant repopulation of the ground state FAD<sub>ox</sub> (which will also contribute to refilling  $1704 \text{ cm}^{-1}$ ). This is not expected if FAD\* decay is exclusively to the FADH<sup>•</sup> intermediate, with ca 300 ps lifetime.  
21 Moreover, the TA data did not clearly show the presence of radical intermediates. Thus, although the TRIR  
22 data can be fit with a single intermediate sequential kinetics, the EADS from TA and TRIR indicate an  
23 underlying complexity, which we ascribe to inhomogeneity in the excited state dynamics, as has been  
24 observed in other BLUF domains [12, 17, 22]. In that case the 33 ps decay of FAD\* is likely better  
25 understood as the mean of a distribution of excited state decay times, some of which lead to FADH<sup>•</sup> while  
26 others are unproductive and recover the ground state or leave FAD\* to decay on the longer time scale  
27 (contributing to SE and ESA in the TA data and the long lived ground state bleach in TRIR). We suggest  
28 this kinetic inhomogeneity reflects the existence of multiple ground state structures around the flavin,  
29 consistent with a dynamic flavin binding site at room temperature.

31

32

33

Frequency	Assignment
1420 (+)	FAD* [17]
1512 (+)	Tyr <sup>•</sup> [45]
1533 (+)	FADH <sup>•</sup> [55]
1547 (-)	FAD [29-31, 56, 57]
1690 (-)	FAD C4=O light adapted state [22, 30]
1704 (-)	FAD C4=O dark adapted state [22, 30]
1704 (+)	E48 (C=O)
1730 (-)	E48 (C=O) [22, 58]

2 Table 1. Frequencies measured by transient infrared absorption and the assignment of the respective  
 3 peaks.

4

5 To complement the study of Q48E OaPAC we also investigated the effect of the replacement of the  
 6 analogous glutamine with a glutamic acid residue in the photochemistry of the BLUF protein Slr 1694  
 7 (PixD); Fig. S3 shows the EADS spectra of this Q50E PixD mutant. The TRIR spectra of the Q50E mutant  
 8 also show the presence of the 1730 cm<sup>-1</sup> mode (indicating that the same hydrogen bonding happens as in  
 9 Q48E OaPAC) as well as the vibrational modes assigned to the neutral tyrosine and flavin radicals. Global  
 10 analysis revealed two components with lifetimes 5ps and 49ps and a third constant component with an  
 11 infinite lifetime describing the kinetics after blue-light excitation of the flavin. The neutral flavin radical is  
 12 formed within ~5ps (Fig. S3). The second EADS shows the characteristic peaks at 1513 cm<sup>-1</sup> and 1531 cm<sup>-1</sup>  
 13 which correspond to vibrational markers of the tyrosine neutral radical and the neutral flavin radical  
 14 (FADH<sup>•</sup>), respectively. The Q50E mutation changes significantly the photochemistry of PixD, as in the  
 15 wild-type protein four components with lifetimes 2.5ps, 20ps, 110ps and 525ps are required to portray the  
 16 dynamics [59]. The photoactivation process in the wild-type protein is sequential, with the formation of the  
 17 anionic flavin radical followed by the stabilization of the neutral flavin radical [27]. In contrast, in the Q50E  
 18 PixD mutant the formation of the FADH<sup>•</sup> and tyrosine neutral radicals are formed with the same time  
 19 constant within 5 ps (Fig. S3) This is similar to the mechanism seen in the Q48E OaPAC mutant. These  
 20 results suggest that the specific mutation in PixD shifts the photochemistry in the direction of a concerted  
 21 PCET (proton coupled electron transfer) and results in a loss of photoactivity in the protein.

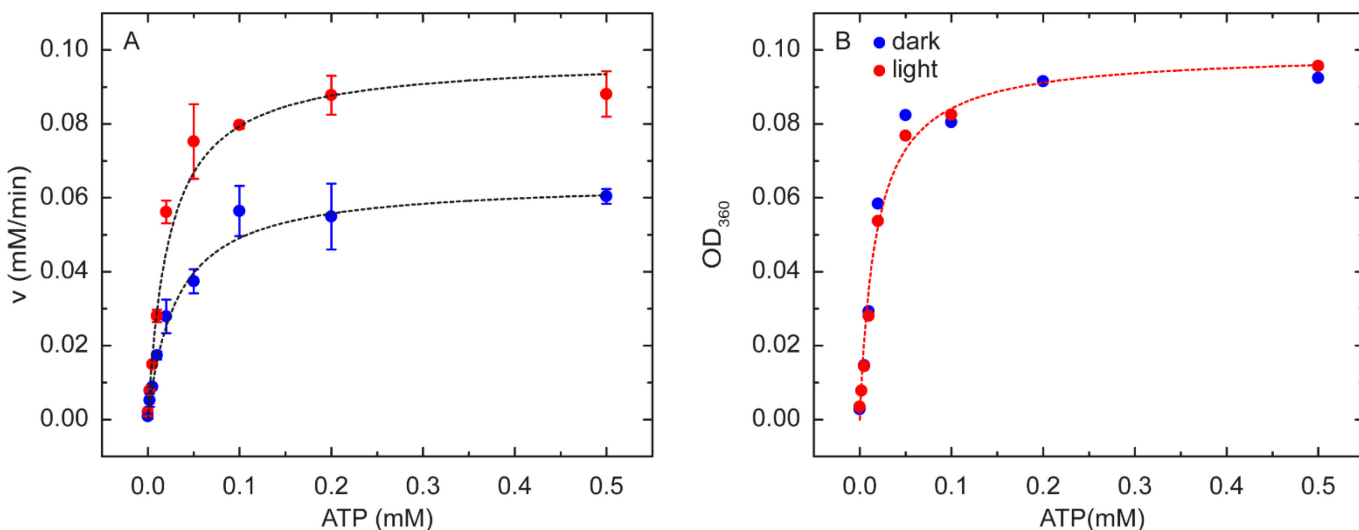
1 *Measurement of ATP-cAMP conversion*

2 We examined the impact of the Q48E mutation on the ability of the AC domain to convert ATP to cAMP.  
3 The ATP to cAMP conversion rate in the Q48E OaPAC mutant was measured using a spectrophotometric  
4 coupled assay as described in the experimental section. Figure 5A shows the enzymatic activity of 2  $\mu$ M  
5 wild-type OaPAC and the 2  $\mu$ M Q48E mutant as a function of ATP concentration. The maximal velocity  
6 of the conversion rate is  $\sim$ 1.5 times higher in the Q48E mutant ( $0.095 \pm 0.003$  mM/min) relative to the WT  
7 protein ( $0.064 \pm 0.001$  mM/min) whereas the concentration of the half-maximal velocity ( $K_M$ ) is  $\sim$ 0.6 lower.  
8 The catalytic constant ( $k_{cat}$ ) which gives the number of substrate molecules that can be converted to cAMP  
9 by the enzyme per unit time is  $\sim$ 1.5 times higher in the Q48E OaPAC ( $47.5 \pm 0.2$  1/min) than in the wild-  
10 type enzyme ( $32.2 \pm 3.5$  1/min) with the enzymatic activity of the light- and dark-adapted state of the Q48E  
11 mutant being the same (Fig. 5B).

12 In the dark, the Q48E mutant shows significant cAMP production compared to the wild-type enzyme, in  
13 which the basal activity is reported to be very low [4, 46]. Turning on the laser at 150 s did not result to an  
14 increase of the cAMP production (Fig. S4).

15 The results of the enzymatic assays are summarized in Table 1. These findings suggest that although the  
16 Q48E mutant is not photoactive (consistent with the absence of the characteristic red-shift in the absorption  
17 spectrum upon blue-light illumination), it has the ability to convert continuously and at a higher rate ATP  
18 to cAMP than wild-type OaPAC. This suggests that the Q48E mutation induces a conformational change  
19 in OaPAC that favours the ATP conversion but suppresses the light-induced changes in the hydrogen bond  
20 network of the flavin.

21



22

1  
2 Fig. 5 A) Michaelis-Menten plot of the enzymatic activity of WT (blue circles) and Q48E (red circles) under irradiation. B)  
3 Michaelis-Menten plot of the enzymatic activity of Q48E without irradiation (blue circles) and under irradiation (red circles)  
4 (the dashed line is the obtained fit). The plot shows that the mutant is in a “switched on” state as light irradiation does not affect  
5 the enzymatic activity.  
6  
7  
8

Kinetic parameters	WT (light)	Q48E dark	Q48E light
$v_{\max}$ (mM min <sup>-1</sup> )	0.064 ± 0.001	0.099 ± 0.004	0.101 ± 0.004
$k_{\text{cat}}$ (min <sup>-1</sup> )	32.2 ± 3.5	49.5 ± 2	50.5 ± 2
$K_M$ (mM)	0.031 ± 0.001	0.018 ± 0.003	0.021 ± 0.002

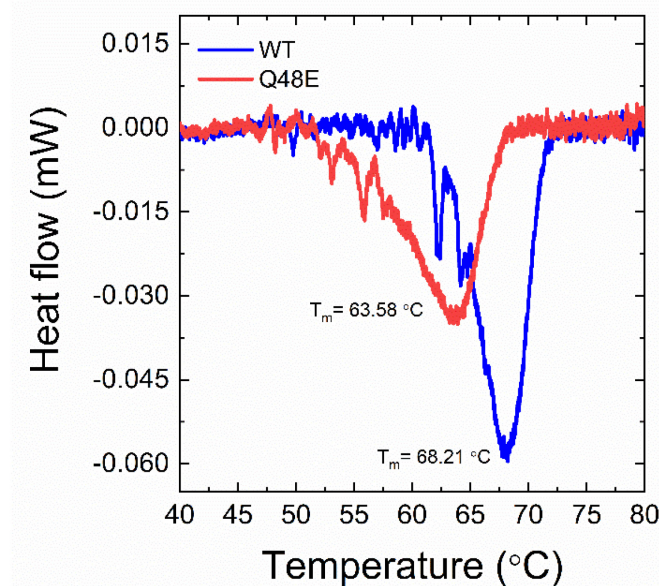
9 Table 2. Enzymatic parameters of light adapted state of WT OaPAC and Q48E in dark and light state  
10  
11  
12  
13  
14

#### *Differential scanning calorimetry (DSC) measurements*

15 As the enzymatic activity of OaPAC changes with the Q48E mutation, suggesting a change in the protein  
16 structure, we performed differential scanning calorimetry measurements to examine the thermostability of  
17 the mutant. Figure 6 shows the heat-flux DSC curves for the wild-type and the Q48E OaPAC in which the  
18 melting temperature ( $T_m$ ) shows where 50% of the protein is denatured whereas the area under the curve  
19 reflects the energy required for protein unfolding associated with the enthalpy change ( $\Delta H$ ). The  
20 measurements reveal significant differences between the wild-type and the mutant OaPAC. In particular,  
21 the thermal denaturation of the wild-type OaPAC shows a steep endothermic unfolding with a  $T_m$  of 68.0°C  
22 and a  $\Delta H$  of 0.078 ± 0.005 J/g. The  $T_m$  of the Q48E OaPAC is significantly lower ( $T_m$  63.6°C) but there is

1 no significant change in the enthalpy of unfolding  $\Delta H$  of  $0.072 \pm 0.005$  J/g. The lower melting temperature  
2 suggests a less compact and more flexible conformation for the Q48E mutant which seem to result to an  
3 increased cAMP production compared to the wild-type OaPAC.

4



5

6 Figure 6. Thermal unfolding of wild-type OaPAC and Q48E OaPAC mutant measured by DSC.

7

8

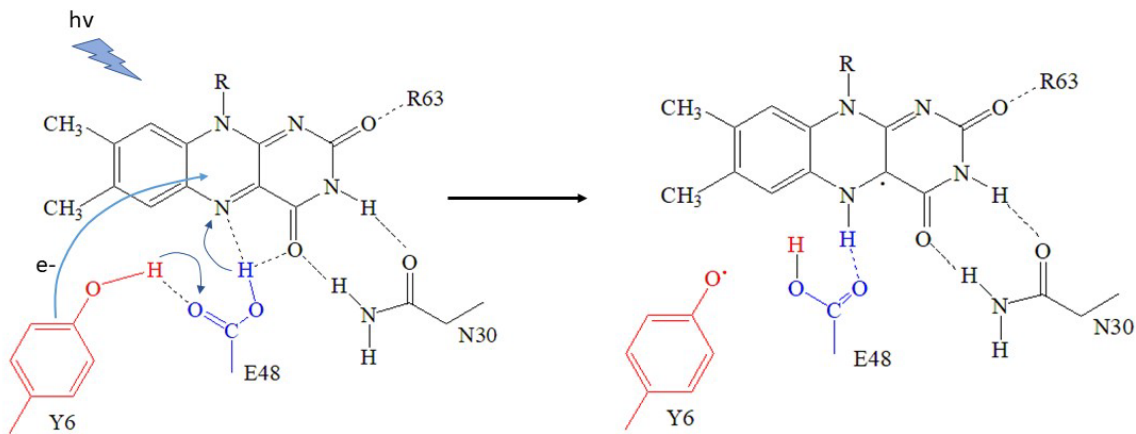
## 9 Conclusions

10 In BLUF domains the functional role of the glutamine residue close to the N5 atom of the flavin has  
11 been investigated extensively, as the mutation of this amino acid in all known BLUF proteins results in a  
12 loss of the photoactivity[16, 21] as well as due to the generally accepted scheme that photoactivation in all  
13 BLUF domains happens via the tautomerisation of this glutamine[16, 22, 34, 36, 60-62].

14 The implications of the replacement of this crucial glutamine was investigated first in AppA, another  
15 BLUF domain protein, by means of transient ultrafast infrared spectroscopy in the case of the Q63L  
16 mutant[16]. TRIR measurements established that in this specific mutant the hydrogen network does not  
17 undergo a reorganization during the photoactivation. The C4=O carbonyl peak of the Q63L mutant does  
18 not shift after excitation compared the to the well-established picture seen in the photoactive BLUF domain

1 where this carbonyl peak shifts from  $\sim 1705$  nm down to  $1685$ - $1690$  nm pointing to hydrogen bond  
2 formation with C4=O[16, 30]. After these measurements Dragnea et al.[21] made the Q63E mutant and  
3 based on UV/VIS and fluorescence spectroscopy measurements proposed that this mutant is in a lit state.  
4 Our TRIR measurements using  $^{13}\text{C}$  labelling showed that glutamic acid (E63) forms a hydrogen bond with  
5 the C4=O carbonyl of flavin either before or together with the excitation [22] resulting in the downshift of  
6 the carbonyl peak in the same way as was observed for the light adapted state of AppA[30]. Dragnea et al.  
7 using size exclusion chromatography observed that the AppA Q63E mutant does not form a complex with  
8 PpsR[21]. As the common understanding was that AppA and PpsR form a complex in the dark and low  
9 oxygen levels but dissociate upon blue light irradiation the authors proposed that AppA Q63E adapts a  
10 structure which keeps the protein in a lit state. This picture was questioned by the finding of the Schlichting  
11 group who observed that the AppA-PpsR complex does not dissociate upon light irradiation[63]. After the  
12 discovery of OaPAC, a photoactivated adenylate cyclase we revisited the role of the mentioned glutamine  
13 as this special BLUF domain protein contains both sensor domain and the effector domain. In this way we  
14 were able to observe the effect of the site directed mutagenesis on the function of the protein directly.

15 Replacement of glutamine with glutamic acid in OaPAC resulted in very similar TRIR spectra to  
16 AppA Q63E and based on the assignment of the peaks we can conclude the following scheme (Fig. 7): the  
17 glutamic acid forms two hydrogen bond with the flavin, one at N5 and one at C4 hence, on excitation we  
18 observe the vibration of the carbonyl of the protonated glutamic acid side chain ( $1730\text{ cm}^{-1}$ ) as well as the  
19 vibrational mode of the C4=O carbonyl ( $\sim 1690\text{ cm}^{-1}$ ); this latter is downshifted compared to the frequency  
20 observed in wild type ( $1704\text{ cm}^{-1}$ ). After excitation the tyrosine (Y6) gives an electron to the flavin and a  
21 proton to the glutamic acid – that might be the origin of the positive  $1704\text{ cm}^{-1}$  peak – and the glutamic acid  
22 gives a proton to the flavin (Grotthus-like mechanism). Observing the individual kinetics at  $1533$  and  $1704$   
23  $\text{cm}^{-1}$  we propose that the protonation of the glutamic acid and the flavin happens within the same time  
24 constant ( $\sim 33\text{ ps}$ ). The individual kinetic data (at  $1533\text{ cm}^{-1}$  and  $1704\text{ cm}^{-1}$ ) as well as the EAS3 show that  
25 the proton and the electron is transferred back in  $346\text{ ps}$  and the flavin relaxes back to it's original (lit) state.



1

2 Figure 7. Photochemistry of flavin and surrounding amino acid due to light absorption. After blue light excitation an electron  
 3 transferred to the flavin and a proton to the glutamic acid in concerted way. A proton is transferred within the same time constant  
 4 to the flavin and the neutral flavin radical is stabilized.

5

6 The structural change caused by the Q48 → E48 mutation is reflected in the UV/VIS and calorimetry  
 7 experiments as well. These latter have shown that the Q48E mutation results in a less compact structure,  
 8 possibly by inducing a structural change in the enzyme as indicated by the ~ 5 °C drop of the melting  
 9 temperature compared to the wild-type OaPAC. These observations suggest that the change in the hydrogen  
 10 network around the flavin (seen in the UV/Vis and the infrared spectra) induces a larger structural change.  
 11 Enzymatic activity assays have proved that this structural change has a substantial impact on the function  
 12 of the enzyme as it converts ATP to cAMP in a light independent manner. Replacement of glutamine to  
 13 glutamic acid resulted in the decoupling of the BLUF domain from AC domain of the protein.

14

15

16

17

18

19

1

2 **Experimental**

3

4 **Materials and methods**

5

6 *Expression and purification of full-length Q48E mutant OaPAC*

7 The wild type and Q48E mutant OaPAC sequences were normalized and purchased from GenScript. The  
8 sequences were inserted into a pET-15b vector in frame with an N-terminal His6-tag under control of a T7  
9 promoter.

10 The purification of proteins were described earlier [64] with some minor changes. Briefly, protein  
11 expression was performed using freshly transformed BL21(DE3) cells. 10 ml Luria broth (LB) medium  
12 containing 10 mg/mL ampicillin was inoculated with a single colony and incubated at 37°C overnight then  
13 used to inoculate 1 L of LB/ampicillin medium in a 4-L flask. The protein expression was induced when  
14 OD600 reached 0.4-0.6 with the addition of 0.7 mM IPTG at 18°C. The harvested and frozen cell pellet  
15 was resuspended in 4x volume lysis buffer with 0.2 mM phenylmethylsulfonyl fluoride (PMSF), DNase,  
16 protease inhibitor cocktail, and lysozyme. The cells were lysed by sonication and cell debris was removed  
17 by centrifugation (12,000 rcf, 1 h). The supernatant was loaded onto a Ni-NTA (Qiagen) column and  
18 incubated it for 1 h at 4°C followed by the elution of protein using 300 mM imidazole. The eluted protein  
19 was dialyzed, and purified to homogeneity using size-exclusion chromatography (Superdex-200).

20 The following buffers were used: lysis buffer (50 mM Na-phosphate buffer, 300 mM NaCl, pH 8.0), wash  
21 buffer (50 mM Na-phosphate buffer, 300 mM NaCl, 5mM imidazole, pH 8.0) elution buffer (50 mM Na-  
22 phosphate buffer, 300 mM NaCl, 300 mM imidazole, pH 8.0), dialysis buffer (50 mM Tris, 150 mM NaCl,  
23 5mM MgCl<sub>2</sub> pH 8.0).

24 *Transient infrared spectroscopy (TRIR)*

25 TRIR spectra were obtained at 20 °C from 100 fs to 3 ns on the ULTRA system at the STFC Central Laser  
26 Facility. The ULTRA system has been described elsewhere [65], and previously used by us to analyse the  
27 photoactivation of AppABLUF [22, 30, 55, 66, 67], and other photoactive and photochromic proteins[68,  
28 69]. Light sensitive samples were analysed using a rastered flow cell, and data were acquired using a 450

1 nm pump pulse operated at 0.2-0.4  $\mu$ J per pulse and a repetition rate of 5 kHz. The spectral resolution was  
2 3 cm<sup>-1</sup> and the temporal resolution was < 200 fs. All samples were prepared at 0.6-0.8 mM concentration  
3 in D<sub>2</sub>O buffer prepared with 20 mM Tris, 150 mM NaCl, pH 8.0. TRIR data were globally analysed using  
4 Glotaran [70][ assuming a sequential scheme with evolutionary associated difference spectra (EADS)  
5 assigned to the obtained time constants[71].

6 *Ultrafast Transient Absorption experiments*

7  
8 Ultrafast transient absorption measurements were performed using a Spitfire Ace regenerative amplifier  
9 system providing ~800  $\mu$ J pulses centered at 800 nm at a repetition rate of 1 kHz. The output of the amplifier  
10 was split in a ratio 1:9. The pulse with the smaller energy was used for the generation of the white light  
11 continuum probe in a CaF<sub>2</sub> crystal. The higher intensity fraction was frequency doubled to 400 nm and  
12 attenuated to ~200-400 nJ/pulse before being used as the pump pulse. Polarization of the probe was set to  
13 the magic angle compared to excitation. To avoid photodegradation the samples were moved with the help  
14 of a Lissajous scanner and simultaneously flowed by a peristaltic pump. Absorption changes were measured  
15 with an Andor CCD and collected with the help of a home written Labview data acquisition software, and  
16 are reported as pump on – pump off normalized difference spectra. The transient absorption dataset was  
17 also globally analysed using the Java based software package Glotaran [70].  
18

19 *cAMP yield measurement / Adenylate Cyclase Activity*

20 The ATP-cAMP conversion of the wild-type and the Q48E OaPAC mutant was quantified using a  
21 pyrophosphate (PPi) assay (EnzChek® Pyrophosphate Assay Kit). The assay is based on the PPi-  
22 dependent conversion of the 2-amino-6-mercaptopurine ribonucleoside (MESG) to ribose  
23 1-phosphate and 2-amino-6-mercaptopurine by the enzyme purine nucleoside phosphorylase  
24 (PNP). The enzymatic conversion of MESG results in a shift in absorbance maximum from 330 to 360 nm.  
25 In addition, the PPi originating from the conversion of ATP to cAMP is catalysed to two equivalents of  
26 phosphate by the enzyme inorganic pyrophosphate present in the assay and enhancing this way the  
27 sensitivity as the phosphate is consumed by the MESG/PNP reaction and the product of the production is  
28 detected by an increase in the absorbance at 360nm. The increase of the absorption at 360 nm was monitored  
29 as a function of time. The reaction rate was determined from the slope of a linear fit using an  
30 extinction coefficient of 11,000 M<sup>-1</sup>cm<sup>-1</sup> at 360 nm.

1 The adenylate cyclase activity of 2  $\mu$ M of WT and Q48E mutant OaPAC was monitored by  
2 continuous illumination with a 473 nm laser light adjusted to a power of 9 mW in the absence and  
3 presence of 500  $\mu$ M of ATP. The reaction rate ( $\mu$ M/s) was determined from the slope of the  
4 absorbance of the purine base product (2-amino-6-mercaptop-7-methylpurine), which is equal to the  
5 reaction rate of pyrophosphate derived from ATP cyclization.

6 To determine the Michaelis-Menten constant, the assay was performed on WT OaPAC and the  
7 Q48E mutant in the presence of 0-500  $\mu$ M concentrations of ATP using the same conditions of  
8 continuous illumination. The initial reaction rate at each ATP concentration was extracted from the  
9 linear portion of OD<sub>360</sub> vs. time plot. The resulting rate constants were plotted as a function of ATP.  
10 By fitting a Michaelis-Menten saturation curve for the enzyme reaction, the maximum reaction rate  
11 ( $V_{max}$ ) and the corresponding  $K_M$  were determined.

12

### 13 *Differential Scanning Calorimetry (DSC) measurements*

14 Differential scanning calorimetry (DSC) was performed to measure the thermal stability of the WT  
15 and Q48E mutant OaPAC using a SETARAM Micro DSC-III calorimeter. The measurements were  
16 carried out in the range of 20 – 100 °C with a heating rate of 0.3 K·min<sup>-1</sup>. The sample (WT and  
17 Q48E) and the reference (buffer solution of WT and Q48E) were balanced with a precision of  $\pm$   
18 0.05 mg in order to avoid corrections with the heat capacity of the vessels. A second thermal scan  
19 of the denatured sample was measured for baseline correction. The melting temperature ( $T_m$ ) of the  
20 thermal unfolding curves were analyzed by the OriginLab Origin®2021 software.

21

### 22 **Author Contributions**

23 J.T.C., Z.F., N.K.B. made the constructs, expressed and purified the proteins. A.L., J.T.C., G.G performed  
24 the infrared transient absorption measurements; A.L., S.R.M., P.J.T. analysed the transient infrared data.  
25 E.B., J.P., M.S. performed the transient absorption measurements. E.B., designed, performed and analysed  
26 the cAMP assays. DSC experiments were performed and analysed by E.T., K.P.U. The project was  
27 conceived by S.R.M, S.M.K., A.L., P.J.T. The manuscript was written by E.B., S.M. K., S.R.M. and A.L.

28

### 29 **Conflicts of interest**

1 “There are no conflicts to declare”.

2 **Acknowledgements**

3 J.T.C. was supported by the National Institutes of Health IMSD-MERGE (T32GM135746) and  
4 NY-CAPs IRACDA (K12-GM102778) Programs at Stony Brook University. A.L. acknowledges  
5 funding from the Hungarian National Research and Innovation Office (K-137557) and was  
6 supported by PTE ÁOK-KA-2021. E.T was supported by PTE ÁOK-KA-2022-09. This study was  
7 supported by the National Science Foundation (NSF) (MCB-1817837 to PJT) and the EPSRC  
8 (EP/N033647/1 to S.R.M.).

9 **Notes and references**

10

- 11 [1] Ohki M, Sugiyama K, Kawai F, Matsunaga S, Iseki M, Park S. Structural basis for photoactivation of a light-regulated adenylate cyclase from  
12 the photosynthetic cyanobacterium *Oscillatoria acuminata*. *Acta Crystallographica a-Foundation and Advances*. 2016;72:S251-S.
- 13 [2] Iseki M, Park SY. Photoactivated Adenylyl Cyclases: Fundamental Properties and Applications. *Adv Exp Med Biol*. 2021;1293:129-39.
- 14 [3] Lindner R, Hartmann E, Tarnawski M, Winkler A, Frey D, Reinstein J, et al. Photoactivation Mechanism of a Bacterial Light-Regulated  
15 Adenylyl Cyclase. *Journal of Molecular Biology*. 2017;429:1336-51.
- 16 [4] Collado J, Iuliano J, Pirisi K, Jewlikar S, Adamczyk K, Greetham G, et al. Unraveling the Photoactivation Mechanism of a Light-Activated  
17 Adenylyl Cyclase Using Ultrafast Spectroscopy Coupled with Unnatural Amino Acid Mutagenesis. *Acs Chemical Biology*. 2022;17:2643-54.
- 18 [5] Lukacs A, Tonge PJ, Meech SR. Photophysics of the Blue Light Using Flavin Domain. *Acc Chem Res*. 2022;55:402-14.
- 19 [6] Gauden M, Yeremenko S, Laan W, van Stokkum I, Ihalaisten J, van Grondelle R, et al. Photocycle of the flavin-binding photoreceptor AppA,  
20 a bacterial transcriptional antirepressor of photosynthesis genes. *Biochemistry*. 2005;44:3653-62.
- 21 [7] Kennis JT, Groot ML. Ultrafast spectroscopy of biological photoreceptors. *Curr Opin Struct Biol*. 2007;17:623-30.
- 22 [8] Fujisawa T, Masuda S. Light-induced chromophore and protein responses and mechanical signal transduction of BLUF proteins. *Biophys  
23 Rev*. 2018;10:327-37.
- 24 [9] Jung A, Reinstein J, Domratcheva T, Shoeman RL, Schlichting I. Crystal structures of the AppA BLUF domain photoreceptor provide insights  
25 into blue light-mediated signal transduction. *J Mol Biol*. 2006;362:717-32.
- 26 [10] Jung A, Domratcheva T, Tarutina M, Wu Q, Ko WH, Shoeman RL, et al. Structure of a bacterial BLUF photoreceptor: insights into blue  
27 light-mediated signal transduction. *Proc Natl Acad Sci U S A*. 2005;102:12350-5.
- 28 [11] Brust R, Lukacs A, Haigney A, Addison K, Gil A, Towrie M, et al. Proteins in action: femtosecond to millisecond structural dynamics of a  
29 photoactive flavoprotein. *J Am Chem Soc*. 2013;135:16168-74.
- 30 [12] Gauden M, Grinstead J, Laan W, van Stokkum I, Avila-Perez M, Toh K, et al. On the role of aromatic side chains in the photoactivation of  
31 BLUF domains. *Biochemistry*. 2007;46:7405-15.
- 32 [13] Bonetti C, Mathes T, van Stokkum IH, Mullen KM, Groot ML, van Grondelle R, et al. Hydrogen bond switching among flavin and amino  
33 acid side chains in the BLUF photoreceptor observed by ultrafast infrared spectroscopy. *Biophys J*. 2008;95:4790-802.
- 34 [14] Bonetti C, Stierl M, Mathes T, van Stokkum I, Mullen K, Cohen-Stuart T, et al. The Role of Key Amino Acids in the Photoactivation Pathway  
35 of the *Synechocystis* Slr1694 BLUF Domain. *Biochemistry*. 2009;48:11458-69.
- 36 [15] Stierl M, Penzkofer A, Kennis J, Hegemann P, Mathes T. Key Residues for the Light Regulation of the Blue Light-Activated Adenylyl Cyclase  
37 from *Beggiatoa* sp. *Biochemistry*. 2014;53:5121-30.
- 38 [16] Stelling AL, Ronayne KL, Nappa J, Tonge PJ, Meech SR. Ultrafast Structural Dynamics in BLUF Domains: Transient Infrared Spectroscopy  
39 of AppA and Its Mutants. *JACS*. 2007;129:15556-64.
- 40 [17] Lukacs A, Brust R, Haigney A, Laptenok SP, Addison K, Gil A, et al. BLUF domain function does not require a metastable radical  
41 intermediate state. *J Am Chem Soc*. 2014;136:4605-15.
- 42 [18] Okajima K, Fukushima Y, Suzuki H, Kita A, Ochiai Y, Katayama M, et al. Fate determination of the flavin photoreceptions in the  
43 cyanobacterial blue light receptor TePixD (TlI0078). *J Mol Biol*. 2006;363:10-8.
- 44 [19] Fukushima Y, Murai Y, Okajima K, Ikeuchi M, Itoh S. Photoreactions of Tyr8- and Gln50-mutated BLUF domains of the PixD protein of  
45 *Thermosynechococcus elongatus* BP-1: photoconversion at low temperature without Tyr8. *Biochemistry*. 2008;47:660-9.
- 46 [20] Yuan H, Anderson S, Masuda S, Dragnea V, Moffat K, Bauer C. Crystal structures of the *Synechocystis* photoreceptor Slr1694 reveal  
47 distinct structural states related to signaling. *Biochemistry*. 2006;45:12687-94.

[21] Dragnea V, Arunkumar A, Lee C, Giedroc D, Bauer C. A Q63E Rhodobacter sphaeroides AppA BLUF Domain Mutant Is Locked in a Pseudo-Light-Excited Signaling State. *Biochemistry*. 2010;49:10682-90.

[22] Lukacs A, Haigney A, Brust R, Zhao RK, Stelling AL, Clark IP, et al. Photoexcitation of the blue light using FAD photoreceptor AppA results in ultrafast changes to the protein matrix. *J Am Chem Soc*. 2011;133:16893-900.

[23] Anderson S, Dragnea V, Masuda S, Ybe J, Moffat K, Bauer C. Structure of a novel photoreceptor, the BLUF domain of AppA from Rhodobacter sphaeroides. *Biochemistry*. 2005;44:7998-8005.

[24] I S. Infrared Spectra and Normal Vibrations of Acetamide and its Deuterated Analogues. *Bulletin of the Chemical Society of Japan*. 1962;35:1279-86.

[25] Sayfutyarova E, Goings J, Hammes-Schiffer S. Electron-Coupled Double Proton Transfer in the Slr1694 BLUF Photoreceptor: A Multireference Electronic Structure Study. *Journal of Physical Chemistry B*. 2019;123:439-47.

[26] Goings J, Hammes-Schiffer S. Early Photocycle of Slr1694 Blue-Light Using Flavin Photoreceptor Unraveled through Adiabatic Excited-State Quantum Mechanical/Molecular Mechanical Dynamics. *Journal of the American Chemical Society*. 2019;141:20470-9.

[27] Gil AA, Laptenok SP, Iuliano JN, Lukacs A, Verma A, Hall CR, et al. Photoactivation of the BLUF Protein PixD Probed by the Site-Specific Incorporation of Fluorotyrosine Residues. *J Am Chem Soc*. 2017;139:14638-48.

[28] Karadi K, Kapetanaki SM, Raics K, Pecsi I, Kapronczai R, Fekete Z, et al. Functional dynamics of a single tryptophan residue in a BLUF protein revealed by fluorescence spectroscopy. *Sci Rep*. 2020;10:2061.

[29] Kondo M, Nappa J, Ronayne K, Stelling A, Tonge P, Meech S. Ultrafast vibrational spectroscopy of the flavin chromophore. *Journal of Physical Chemistry B*. 2006;110:20107-10.

[30] Haigney A, Lukacs A, Zhao RK, Stelling AL, Brust R, Kim RR, et al. Ultrafast infrared spectroscopy of an isotope-labeled photoactivatable flavoprotein. *Biochemistry*. 2011;50:1321-8.

[31] Wolf MM, Schumann C, Gross R, Domratcheva T, Diller R. Ultrafast infrared spectroscopy of riboflavin: dynamics, electronic structure, and vibrational mode analysis. *J Phys Chem B*. 2008;112:13424-32.

[32] Wolf MM, Zimmermann H, Diller R, Domratcheva T. Vibrational mode analysis of isotope-labeled electronically excited riboflavin. *J Phys Chem B*. 2011;115:7621-8.

[33] Haigney A, Lukacs A, Brust R, Zhao RK, Towrie M, Greetham GM, et al. Vibrational assignment of the ultrafast infrared spectrum of the photoactivatable flavoprotein AppA. *J Phys Chem B*. 2012;116:10722-9.

[34] Hontani Y, Mehlhorn J, Domratcheva T, Beck S, Kloz M, Hegemann P, et al. Spectroscopic and Computational Observation of Glutamine Tautomerization in the Blue Light Sensing Using Flavin Domain Photoreaction. *J Am Chem Soc*. 2023;145:1040-52.

[35] Gauden M, van Stokkum I, Key J, Luhrs D, Van Grondelle R, Hegemann P, et al. Hydrogen-bond switching through a radical pair mechanism in a flavin-binding photoreceptor. *Proceedings of the National Academy of Sciences of the United States of America*. 2006;103:10895-900.

[36] Sadeghian K, Bocola M, Schütz M. A conclusive mechanism of the photoinduced reaction cascade in blue light using flavin photoreceptors. *J Am Chem Soc*. 2008;130:12501-13.

[37] Chen Z, Kang XW, Zhou Y, Zhou Z, Tang S, Zou S, et al. Dissecting the Ultrafast Stepwise Bidirectional Proton Relay in a Blue-Light Photoreceptor. *J Am Chem Soc*. 2023;145:3394-400.

[38] AGMON N. THE GROTHUSS MECHANISM. *Chemical Physics Letters*. 1995;244:456-62.

[39] Sun M, Moore TA, Song PS. Molecular luminescence studies of flavins. I. The excited states of flavins. *J Am Chem Soc*. 1972;94:1730-40.

[40] Konold PE, Arik E, Weißenborn J, Arents JC, Hellingwerf KJ, van Stokkum IHM, et al. Confinement in crystal lattice alters entire photocycle pathway of the Photoactive Yellow Protein. *Nat Commun*. 2020;11:4248.

[41] TONGE P, MOORE G, WHARTON C. FOURIER-TRANSFORM INFRARED STUDIES OF THE ALKALINE ISOMERIZATION OF MITOCHONDRIAL CYTOCHROME-C AND THE IONIZATION OF CARBOXYLIC-ACIDS. *Biochemical Journal*. 1989;258:599-605.

[42] FAHMY K, JAGER F, BECK M, ZVYAGA T, SAKMAR T, SIEBERT F. PROTONATION STATES OF MEMBRANE-EMBEDDED CARBOXYLIC-ACID GROUPS IN RHODOPSIN AND METARHODOPSIN-II - A FOURIER-TRANSFORM INFRARED-SPECTROSCOPY STUDY OF SITE-DIRECTED MUTANTS. *Proceedings of the National Academy of Sciences of the United States of America*. 1993;90:10206-10.

[43] Lubben M, Gerwert K. Redox FTIR difference spectroscopy using caged electrons reveals contributions of carboxyl groups to the catalytic mechanism of haem-copper oxidases. *Febs Letters*. 1996;397:303-7.

[44] Dioumaev A. Infrared methods for monitoring the protonation state of carboxylic amino acids in the photocycle of bacteriorhodopsin. *Biochemistry-Moscow*. 2001;66:1269-76.

[45] Pirisi K, Nag L, Fekete Z, Iuliano JN, Tolentino Collado J, Clark IP, et al. Identification of the vibrational marker of tyrosine cation radical using ultrafast transient infrared spectroscopy of flavoprotein systems. *Photochem Photobiol Sci*. 2021;20:369-78.

[46] Ohki M, Sugiyama K, Kawai F, Tanaka H, Nihei Y, Unzai S, et al. Structural insight into photoactivation of an adenylate cyclase from a photosynthetic cyanobacterium. *Proceedings of the National Academy of Sciences of the United States of America*. 2016;113:6659-64.

[47] Zhou Z, Chen Z, Kang XW, Zhou Y, Wang B, Tang S, et al. The nature of proton-coupled electron transfer in a blue light using flavin domain. *Proc Natl Acad Sci U S A*. 2022;119:e2203996119.

[48] DIXON W, MURPHY D. DETERMINATION OF ACIDITY CONSTANTS OF SOME PHENOL RADICAL CATIONS BY MEANS OF ELECTRON-SPIN RESONANCE. *Journal of the Chemical Society-Faraday Transactions I*. 1976;72:1221-30.

[49] Solar S, Gtoff N, Surdhar PS, Armstrong DA, Singh A. Oxidation of tryptophan and N-methylindole by N3<sup>•</sup>, Br2<sup>•-</sup> and (SCN)2<sup>•-</sup> radicals in light- and heavy-water solutions: a pulse radiolysis study. *Journal of Physical Chemistry* 1991. p. 3639-43.

[50] Nag L, Sournia P, Myllykallio H, Liebl U, Vos M. Identification of the TyrOH(center dot+) Radical Cation in the Flavoenzyme TrmFO (vol 139, pg 11500, 2017). *Journal of the American Chemical Society*. 2017;139:15554-.

[51] Nag L, Lukacs A, Vos MH. Short-Lived Radical Intermediates in the Photochemistry of Glucose Oxidase. *Chemphyschem*. 2019;20:1793-8.

1 [52] Pirisi K, Nag L, Fekete Z, Iuliano JN, Collado JT, Clark IP, et al. Identification of the vibrational marker of tyrosine cation radical using  
2 ultrafast transient infrared spectroscopy of flavoprotein systems. *Photochem Photobiol Sci.* 2021;20:369-78.

3 [53] Green D, Roy P, Hall CR, Iuliano JN, Jones GA, Lukacs A, et al. Excited State Resonance Raman of Flavin Mononucleotide: Comparison of  
4 Theory and Experiment. *J Phys Chem A.* 2021;125:6171-9.

5 [54] Goings JJ, Reinhardt CR, Hammes-Schiffer S. Propensity for Proton Relay and Electrostatic Impact of Protein Reorganization in Slr1694  
6 BLUF Photoreceptor. *JACS.* 2018;140:15241-51.

7 [55] Lukacs A, Zhao RK, Haigney A, Brust R, Greetham GM, Towrie M, et al. Excited state structure and dynamics of the neutral and anionic  
8 flavin radical revealed by ultrafast transient mid-IR to visible spectroscopy. *J Phys Chem B.* 2012;116:5810-8.

9 [56] Haigney A, Kondo M, Stelling A, Lukacs A, Bacher A, Tonge P, et al. Determining Structural Differences in the Dark and Light States of  
10 AppA using Vibrational and Ultrafast Fluorescence Spectroscopy. *Faseb Journal.* 2010;24.

11 [57] Zhu J, Mathes T, Stahl AD, Kennis JT, Groot ML. Ultrafast mid-infrared spectroscopy by chirped pulse upconversion in 1800-1000cm(-1)  
12 region. *Opt Express.* 2012;20:10562-71.

13 [58] Hense A, Herman E, Oldemeyer S, Kottke T. Proton Transfer to Flavin Stabilizes the Signaling State of the Blue Light Receptor Plant  
14 Cryptochrome. *Journal of Biological Chemistry.* 2015;290:1743-51.

15 [59] Gil AA, Laptenok SP, Iuliano JN, Lukacs A, Verma A, Hall CR, et al. Photoactivation of the BLUF Protein PixD Probed by the Site-Specific  
16 Incorporation of Fluorotyrosine Residues. *JACS.* 2017;139:14638-48.

17 [60] Khrenova MG, Domratcheva T, Schlichting I, Grigorenko BL, Nemukhin AV. Computational characterization of reaction intermediates in  
18 the photocycle of the sensory domain of the AppA blue light photoreceptor. *Photochem Photobiol.* 2011;87:564-73.

19 [61] Khrenova MG, Nemukhin AV, Domratcheva T. Photoinduced electron transfer facilitates tautomerization of the conserved signaling  
20 glutamine side chain in BLUF protein light sensors. *J Phys Chem B.* 2013;117:2369-77.

21 [62] Hsiao YW, Götze JP, Thiel W. The central role of Gln63 for the hydrogen bonding network and UV-visible spectrum of the AppA BLUF  
22 domain. *J Phys Chem B.* 2012;116:8064-73.

23 [63] Winkler A, Heintz U, Lindner R, Reinstein J, Shoeman RL, Schlichting I. A ternary AppA-PpsR-DNA complex mediates light regulation of  
24 photosynthesis-related gene expression. *Nat Struct Mol Biol.* 2013;20:859-67.

25 [64] Kapetanaki SM, Fekete Z, Dorlet P, Vos MH, Liebl U, Lukacs A. Molecular insights into the role of heme in the transcriptional regulatory  
26 system AppA/PpsR. *Biophys J.* 2022;121:2135-51.

27 [65] Greetham G, Burgos P, Cao Q, Clark I, Codd P, Farrow R, et al. ULTRA: A Unique Instrument for Time-Resolved Spectroscopy. *Applied  
28 Spectroscopy.* 2010;64:1311-9.

29 [66] Zhao RK, Lukacs A, Haigney A, Brust R, Greetham GM, Towrie M, et al. Ultrafast transient mid IR to visible spectroscopy of fully reduced  
30 flavins. *Phys Chem Chem Phys.* 2011;13:17642-8.

31 [67] Haigney A, Lukacs A, Brust R, Zhao R, Towrie M, Greetham G, et al. Vibrational Assignment of the Ultrafast Infrared Spectrum of the  
32 Photoactivatable Flavoprotein AppA. *Journal of Physical Chemistry B.* 2012;116:10722-9.

33 [68] Lukacs A, Haigney A, Brust R, Addison K, Towrie M, Greetham GM, et al. Protein photochromism observed by ultrafast vibrational  
34 spectroscopy. *J Phys Chem B.* 2013;117:11954-9.

35 [69] Laptenok SP, Lukacs A, Gil A, Brust R, Sazanovich IV, Greetham GM, et al. Complete Proton Transfer Cycle in GFP and Its T203V and S205V  
36 Mutants. *Angew Chem Int Ed Engl.* 2015;54:9303-7.

37 [70] Snellenburg J, Laptenok S, Seger R, Mullen K, van Stokkum I. Glotaran: A Java-Based Graphical User Interface for the R Package TIMP.  
38 *Journal of Statistical Software.* 2012;49:1-22.

39 [71] van Stokkum IH, Larsen DS, van Grondelle R. Global and target analysis of time-resolved spectra. *Biochim Biophys Acta.* 2004;1657:82-  
40 104.